*Acta Oceanol. Sin.*, 2021, Vol. 40, No. 2, P. 136–146
https://doi.org/10.1007/s13131-021-1758-6
http://www.hyxb.org.cn
E-mail: hyxbe@263.net

# An insight into shallow gas hydrates in the Dongsha area, South China Sea

Bin Liu[1], Jiangxin Chen[2, 3]*, Luis M. Pinheiro[4], Li Yang[1], Shengxuan Liu[1], Yongxian Guan[1], Haibin Song[5], Nengyou Wu[2, 3], Huaning Xu[2, 3], Rui Yang[2, 3]

[1] Key Laboratory of Marine Mineral Resources, Ministry of Natural Resources, Guangzhou Marine Geological Survey, Guangzhou 510075, China

[2] Key Laboratory of Gas Hydrate, Ministry of Natural Resources, Qingdao Institute of Marine Geology, Qingdao 266071, China

[3] Laboratory for Marine Mineral Resources, Pilot National Laboratory for Marine Science and Technology (Qingdao), Qingdao 266237, China

[4] Departamento de Geociências and Centre for Environmental and Marine Studies, Universidade de Aveiro, Aveiro 3800, Portugal

[5] State Key laboratory of Marine Geology, Tongji University, Shanghai 200092, China

Received 16 January 2020; accepted 16 June 2020



**Abstract**

Previous studies of gas hydrate in the Dongsha area mainly focused on the deep-seated gas hydrates that have a high energy potential, but cared little about the shallow gas hydrates occurrences. Shallow gas hydrates have been confirmed by drill cores at three sites (GMGS2 08, GMGS2 09 and GMGS2 16) during the GMGS2 cruise, which occur as veins, blocky nodules or massive layers, at 8–30 m below the seafloor. Gas chimneys and faults observed on the seismic sections are the two main fluid migration pathways. The deep-seated gas hydrate and the shallow hydrate-bearing sediments are two main seals for the migrating gas. The occurrences of shallow gas hydrates are mainly controlled by the migration of fluid along shallow faults and the presence of deep-seated gas hydrates. Active gas leakage is taking place at a relatively high-flux state through the vent structures identified on the geophysical data at the seafloor, although without resulting in gas plumes easily detectable by acoustic methods. The presence of strong reflections on the high-resolution seismic profiles and dim or chaotic layers in the sub-bottom profiles are most likely good indicators of shallow gas hydrates in the Dongsha area. Active cold seeps, indicated by either gas plume or seepage vent, can also be used as indicators for neighboring shallow gas hydrates and the gas hydrate system that is highly dynamic in the Dongsha area.

**Key words:** shallow gas hydrate, Dongsha, cold seep, fluid flow, methane-derived authigenic carbonate, South China Sea

**Citation:** Liu Bin, Chen Jiangxin, Pinheiro Luis M., Yang Li, Liu Shengxuan, Guan Yongxian, Song Haibin, Wu Nengyou, Xu Huaning, Yang Rui. 2021. An insight into shallow gas hydrates in the Dongsha area, South China Sea. Acta Oceanologica Sinica, 40(2): 136–146, doi: 10.1007/s13131-021-1758-6

## 1 Introduction

Gas hydrates are ice-like compound of water and methane (or higher hydrocarbons). Gas hydrates are formed under low temperature and high pressure conditions. They represent a potential important energy source and they contain a large amount of carbon (Boswell and Collett, 2011). They may have greatly contributed to the past climate changes, considering their facility to decompose in response to changes of temperature or pressure and their potential to release massive amounts of methane, a potential greenhouse gas, into the upper hydrosphere and atmosphere (Kvenvolden, 1993; Etiope et al., 2008; Reagan and Moridis, 2007; Ruppel and Kessler, 2017). Gas hydrates are also highly significant as concerns seafloor stability, given their potential to fluidize sediments by dissociation and produce submarine landslides (Vanneste et al., 2014). Although gas hydrates can be found onshore at high latitudes, most gas hydrates occur in marine settings. They occur as large-scale gas hydrates distributed near the lower boundary of the gas hydrate stability zone (GHSZ), and as localized gas hydrates concentrated near the seafloor (Riedel et al., 2006; Bahk et al., 2009). Near-seafloor gas hydrates form a small amount of the total gas hydrates, but they play a significant role in helping to better understand how gas hydrate respond to environmental changes (Suess et al., 2001). Moreover, shallow gas hydrates (SGH) provide new insights into the migration of hydrocarbon-rich fluids to the seabed and their role in sustaining deep sea communities and ecosystems (Foucher et al., 2009; Wenau et al., 2015).

SGH have been documented in many oceans around the world, such as the Ulleung Basin in Korea (Bahk et al., 2009), the Cascadia margin (Riedel et al., 2006), the Gulf of Mexico (Mac-

Foundation item: The Laboratory for Marine Mineral Resources, Qingdao National Laboratory for Marine Science and Technology under contract No. MMRKF201810; the National Key Research & Development Program of China under contract Nos 2018YFC0310000 and 2017YFC0307406; the Shandong Province "Taishan Scholar" Construction Project.
*Corresponding author, E-mail: jiangxin_chen@sina.com

Donald et al., 1994) and the Gulf of Cadiz (Gardner, 2001; Mazurenko et al., 2002; Pinheiro et al., 2003). Some of these sites have been the focus of extensive investigations and continuous monitoring. MacDonald et al. (2005) used continuous monitoring, remote operated vehicles and sediment sampling to study the SGH on the Bush Hill and were able to better understand how gas hydrates respond to the tidal and water temperature changes. Riedel et al. (2006) conducted a multi-disciplinary survey on the SGH in the Bullseye cold seep, Cascadia, and proposed a model supported by time-lapse data. In this model, faults and fractures formed in new place provide new pathways for fluid migration and facilitate the formation of SGH in new areas (Riedel, 2007).

Relatively well-established methods have been proposed to explore the deep-seated gas hydrates. The seismic method, among them, is the most successfully and widely used. Bottom simulating reflectors (BSRs) identified on seismic reflection profiles have been long used to predict the existence of gas hydrates (Shipley et al., 1979; Berndt et al., 2004; Petersen et al., 2007; Shedd et al., 2012). The BSRs mimic the seafloor, often have a strong amplitude with reverse polarity, and are considered to correspond to the lower boundary of GHSZ, separating the gas hydrate-bearing sediments above from the free gas-bearing sediment below (Bangs et al., 1993; MacKay et al., 1994; Hyndman and Spence, 1992). Additionally, the acoustic impedance, velocity and amplitude anomalies are also frequently used to study the deep-seated gas hydrate (Boswell et al., 2016). However, detection of shallow gas hydrate is much more difficult.

Multiple drilling programs conducted by the Guangzhou Marine Geological Survey (GMGS), such as GMGS 1–4 proved the widespread distribution of gas hydrates in the northern slope of the South China Sea (Zhang et al., 2007, 2014; Yang et al., 2015). Previous work in this area, however, mainly focused on the deep-seated gas hydrates, with an energy source perspective, and much less attention has been given to the near-seafloor gas hydrates. Nevertheless, the first offshore natural gas hydrate production test has confirmed a complex gas hydrate system in the adjacent area (Li et al., 2018). In this study, available multiple datasets are analyzed, including multi-channel seismics (MCS), sub-bottom profiler (SBP) sections and drilling results, to investigate the occurrences of SGH at three sites (Fig. 1). The study aims to (1) characterize the shallow gas hydrate using geophysical and logging data, (2) identify and better understand the fluid migration pathways in the Dongsha area, (3) better detect and recognize these occurrences, inferring exploration indicators for SGH, and (4) discuss the relationship between the widely distributed cold seeps and SGH, in order to better understand the dynamic processes involved, crucial for the future exploration and exploitation of gas hydrate in the Dongsha area.

## 2 Geological setting

The study sites are located in the Dongsha area, in the northeastern slope of the South China Sea (Fig. 1). The water depth in this area is highly variable, within a depth range of 500 to 2 200 m. The sea bottom morphology is very complex with a lot of chan-

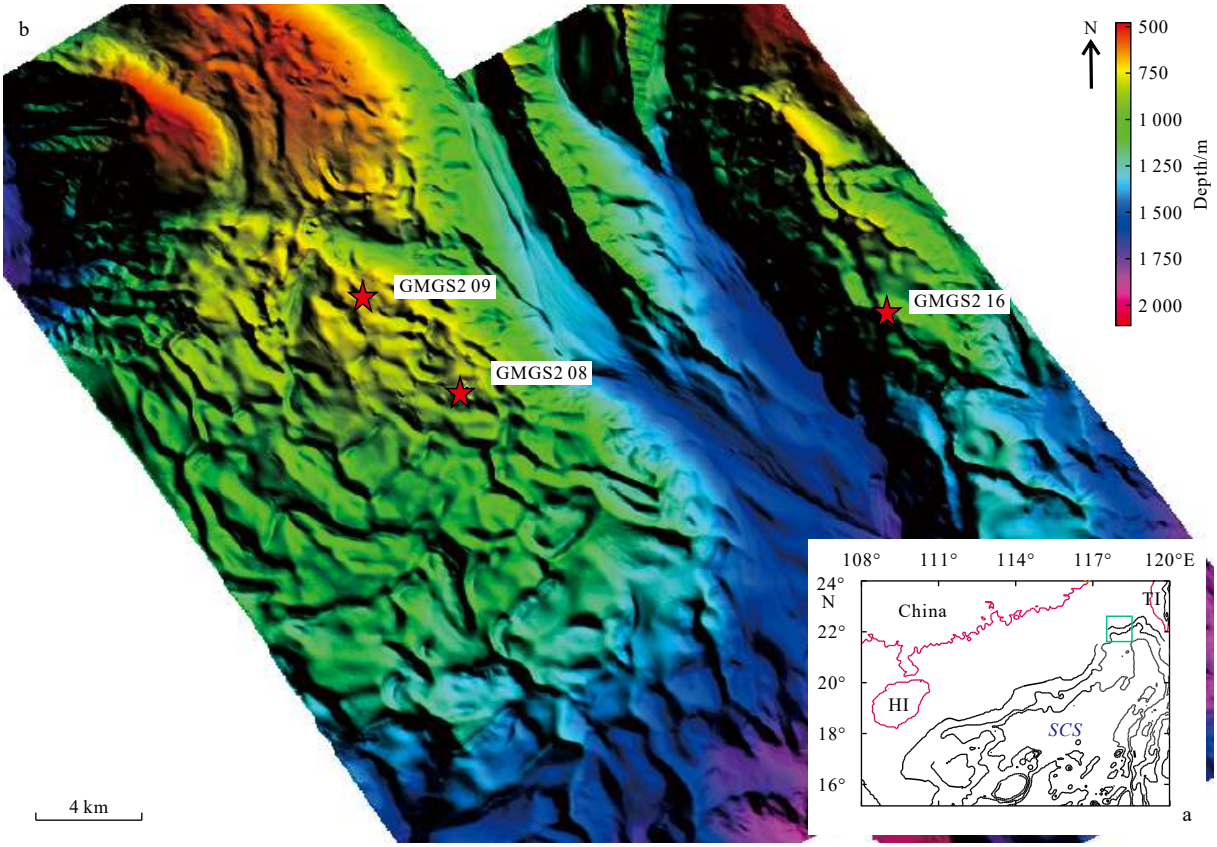


**Fig. 1.** The map shows the location of the study area, which is the target area of the GMGS2 drilling program. The inset with the site location in a broader area is modified from Zhang et al. (2014). The shallow gas hydrates (SGH) close to the seafloor were recovered from the drill cores at sites GMGS2 08 (site 08), GMGS2 09 (site 09) and GMGS2 16 (site 16) (red stars). Site 08 and site 09 are within the Jiulong methane reef zone which was discovered in 2004 (Chen et al., 2005; Han et al., 2008). HI: Hainan Island, TI: Taiwan Island, SCS: South China Sea. The green rectangle in a indicates the study area and the grid interval of multi-beam bathymetric data is 50 m.

nels, seamounts, canyons and sea knolls. Among them, the submarine canyons trending from NW to SE and extending from the upper shelf to the lower slope transport large amount of sediments to the slope and rise (Sha et al., 2015; Wang et al., 2018c). This area is also home to many mud diapirs and faults. Some faults penetrate the basin base and some faults reach the seafloor, which favor the migration of methane and higher hydrocarbons and the formation of gas hydrates (Shyu et al., 1998; Yan et al., 2006).

Many previous studies demonstrated that the Dongsha area is promising for gas hydrates, particularly considering the high sedimentation rate and the tectonic setting (McDonnell et al., 2000). BSRs, a widely used indicator of gas hydrates has also been reported (Li et al., 2013). Cold seep sites and methane-derived carbonate discovered during the R/V *SONNE 177* Cruise in 2004 (Han et al., 2008), also suggested the existence of gas hydrates. The GMGS2 drilling program finally recovered gas hydrates samples in this area (Zhang et al., 2014). Along with the gas hydrates distributed close to the lower boundary of GHSZ, SGHs were recovered at three sites: GMGS2 08, GMGS2 09 and GMGS2 16. Using site 08, site 09 and site 16 for short (Sha et al., 2015) (Fig. 1).

The first discovery of the widespread methane-derived authigenic carbonates (MDAC) in the Jiulong methane reef, in 2004 (Chen et al., 2005, 2006; Han et al., 2008, 2014) was followed by many other similar discoveries and research studies (Lu et al., 2005; Huang et al., 2006; Wang et al., 2012, 2014b). These works make the South China Sea an important area for the study of the methane seepage and further indicate that gas hydrates may be widespread. Moreover, a recent study shows that gas seepages are associated with the gas hydrate accumulations here (Wang et al., 2018d). Most of the work carried out in this area focused on the understanding the past episodes of the methane seepage (Chen et al., 2016; Li et al., 2016), the source of the hydrocarbon-rich fluids (Feng and Chen, 2015) and the possible relationship between the dissociation of gas hydrate and the seepages of methane through geochemical analysis of the MDAC (Zhuang et al., 2016). The U/Th dating of the seep carbonate and seep bivalve fragments shows that all events of methane seepage occurred between (11.5±0.2) ka and (144.5±12.7) ka and the methane seepage events correspond to the lower sea-level periods (Han et al., 2014).

## 3 Materials and methods

The datasets used in this work include sub-bottom profiles, high-resolution 3D multi-channel seismic data, drill cores and logs. The geophysical data were acquired during several cruises in 2011 and 2012. The well logs were recorded during the GMGS-2 drilling project launched in 2013.

### 3.1 *Sub-bottom profiler data*

The sub-bottom profiler data were collected in 2012, using a Parasound P70 system from Teledyne RESON, hull-mounded on the Haiyang 6 Research Vessel. The system uses parametric effect to generate secondary signals. A low frequency secondary signal is achieved by transmitting two primary high frequency signals. The primary high frequency used is 18 kHz and the secondary low frequency is 4 kHz. The system operates at a pulse model with a pulse length of 1.5 ms. The sampling rate is 0.3 ms. Along track data points are typically 3–4 m apart. Both the envelope and waveform data were recorded, but only the latter was used. The waveform data were processed using the Radexpro software.

### 3.2 *3D high-resolution seismic data*

The 3D seismic data used in this study were acquired in 2011. An array of generator injector guns source was used as the source. The source has a total volume of 0.008 9 $m^3$. It generates a seismic energy pulse with frequencies from 10–150 Hz. The dominant frequency is about 65 Hz. The dominant wavelength is about 25 m and the vertical resolution is about 6 m, assuming a seismic velocity is 1 600 m/s for the shallow sedimentary section. The 3D seismic data were created from closely spaced 2D lines. The shot line spacing was 100 m and the shot spacing was 12.5 m. The streamer had 768 channels with an interval between active sections of 3.125 m.

This 3D dataset has been processed commercially following a typical industry workflow. The data were high-pass filtered with a low frequency limit of 3–6 Hz. Frequency dependent methods were used to attenuate noise. Multiples were attenuated in 3D. The bin size used is 3.125 m×50 m. Routine normal move-out approach was used to build the velocity model needed by the following migration procedure. Pre-stack time migration was used to produce the subsurface images.

### 3.3 *Well logs and drilling cores*

The GMGS2 expedition was launched by the Chinese Geological Survey in 2013, with the collaboration of Fugro and Geotek. The aim of the GMGS2 drilling program is to quantify the gas hydrates in the sediment cores and to determine the nature and distribution of gas hydrates in this area. Cores were acquired by using Fugro Hydraulic Piston Corer. The velocity, density and resistivity logs were obtained through the Logging while drilling technique. More detailed and comprehensive information about the GMGS2 program can be found in Sha et al. (2015).

### 3.4 *Synthetic seismograms*

Impedance contrast profiles were obtained from the velocity and density logs, and synthetic seismograms were obtained through convolution of the reflection coefficients with a source wavelet. Here, the wavelet was extracted from the seismic data.

## 4 Results

### 4.1 *Drilling and logging observations*

The drill cores revealed the presence of SGH close to the seafloor at three sites: site 08, site 09 and site 16. Gas hydrate samples occur in the form of massive layers, veins or blocky nodules, at the depth interval 8–30 m (Table 1). MDAC were recovered at sites 08 and 09. At site 08, a 3 m thick MDAC occurs

**Table 1.** Information on the shallow gas hydrates layers from drilling results

| Site | Water depth/m | Depth below seafloor/m | Distribution type | Resistivity/Ω·m | Seismic velocity/(m·s$^{-1}$) | Methane-derived authigenic carbonates |
|---|---|---|---|---|---|---|
| 08 | 801 | 8–23 | massive layer, vein, or blocky nodule | 15 | up to 1 650 | localized at shallow depth |
| 09 | 727 | 9–21 | nodule | 1.2 | around 1 550 | abundant on the seafloor |
| 16 | 879 | 15–30 | nodule | 27 | up to 1 650 | none |

just above the top of the SGH zone. At below seafloor 58–63 m, another MDAC formation occurs. At site 09, the seafloor hosts abundant MDAC.

The depth profiles of the concentrations of the ion sulfate ($SO_4^{2-}$) and methane ($CH_4$) in pore water at site 08 and site 16 are displayed in Fig. 2. Such depth profiles are not observed at site 09. The sulfate methane interface (SMI) depths are at 5 m and 8 m below the seafloor, at site 08 and site 16 respectively, based on the gradient of the concentration of the ion sulfate.

The well logs at the three sites are displayed in Figs 3–5. High

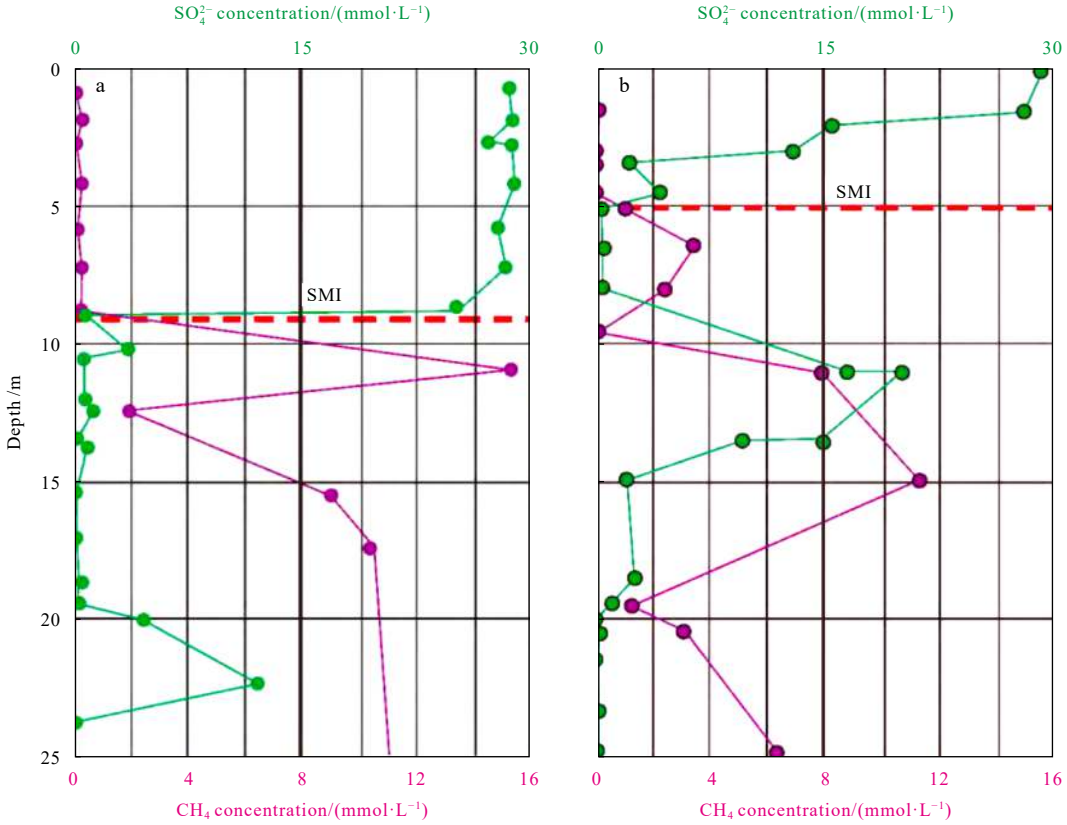


**Fig. 2.** Depth profiles of sulfate and methane concentration in pore water in sediments from the drill cores at site 16 (a) and site 08 (b). Note the sulfate methane interfaces in a and b. SMI is sulfate methane interface.

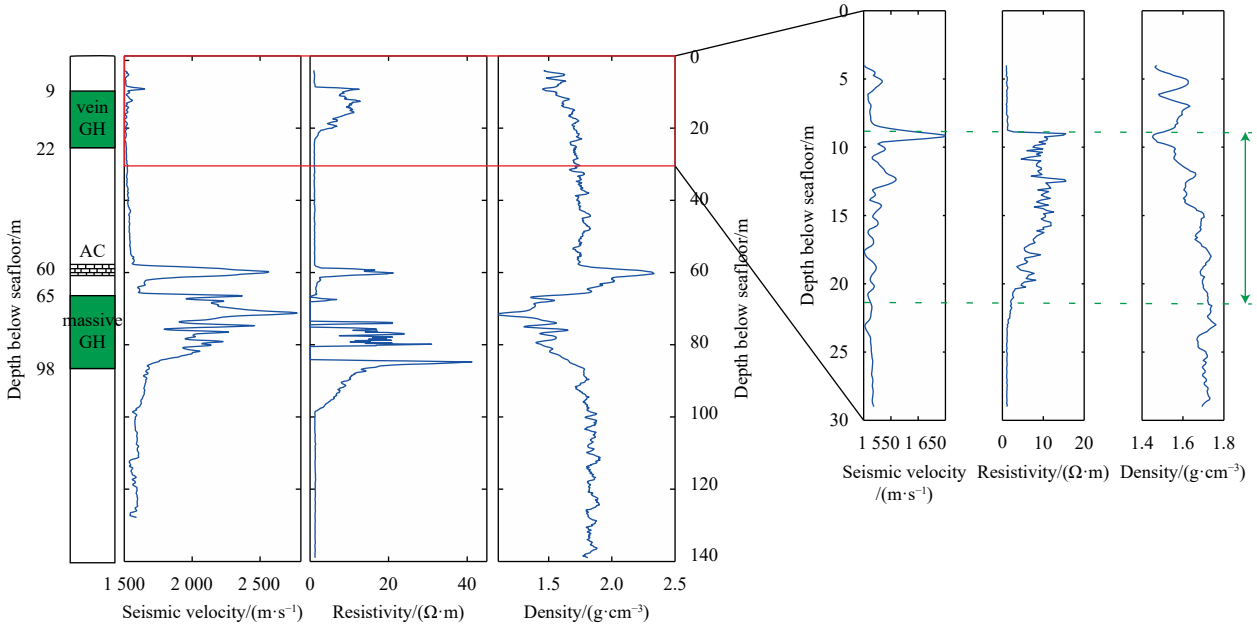


**Fig. 3.** Logging while drilling data at site 08. Shallow gas hydrates are concentrated at depth below seafloor 9–22 m (green line with arrows). GH: gas hydrate, AC: authigenic carbonate.

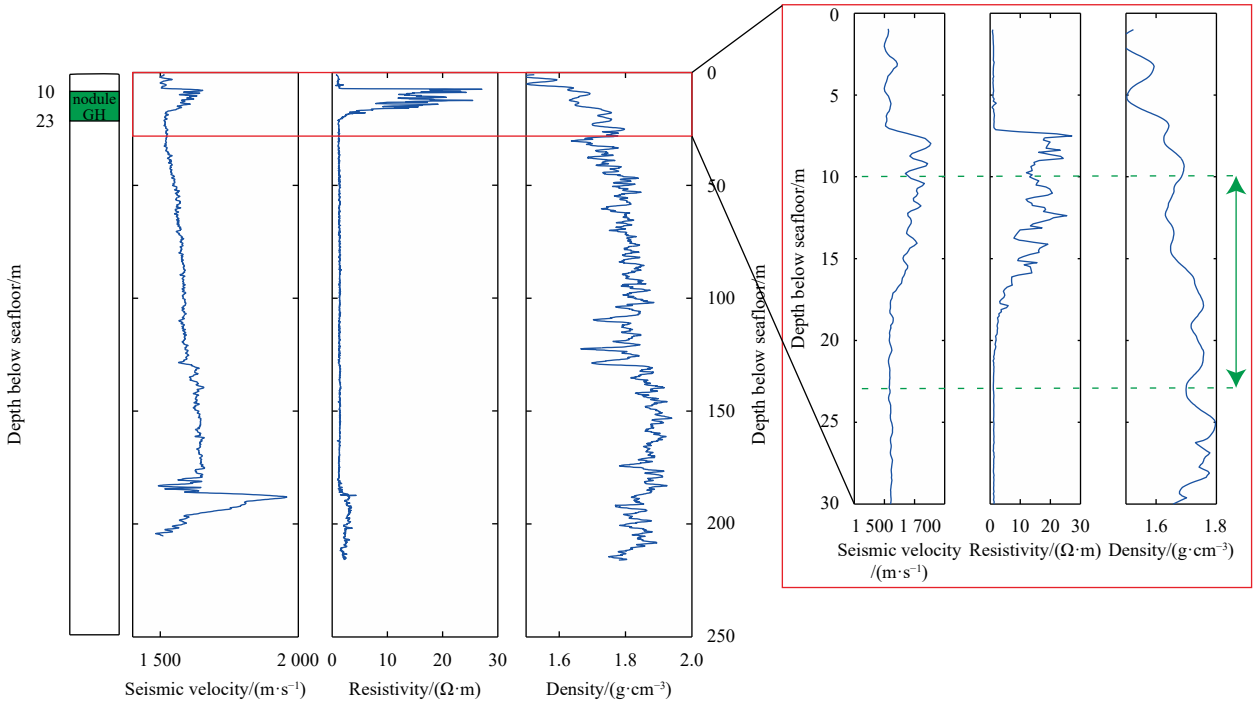


**Fig. 4.** Logging while drilling data at site 16. Shallow gas hydrates are concentrated at depth below seafloor 10–23 m (green line with arrows). GH: gas hydrate.

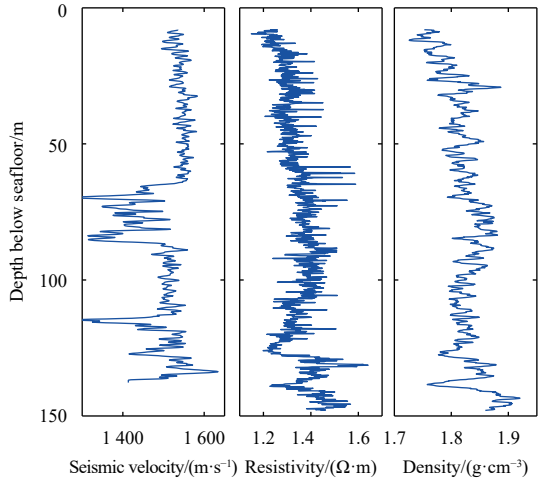


**Fig. 5.** Logging while drilling data at site 09. Shallow gas hydrates are concentrated at depth below seafloor 9–21 m. Note that data is not recorded in the shallow layer.

seismic velocity and high resistivity zones are observed at both sites 08 and 16. At site 08, the resistivity of the SGH zone is up to 17 Ω·m, while the background resistivity is about 1.2 Ω·m. The seismic velocity is up to 1 650 m/s at 10 m below the seafloor, while the background velocity is about 1 540 m/s (Fig. 3). Site 16 has similar characteristics to site 08, with two anomalous zones. The resistivity of the SGH zone is up to 27 Ω·m (Fig. 4). At site 09, however, the log characteristics are quite different from sites 08 and 16 with no anomaly being observed neither on the velocity nor on the resistivity log (Fig. 5).

### 4.2 *Geophysical characteristics*

Site 08 was drilled on the flank of a small mound. The water depth of the drilling site is about 801 m (Fig. 6a). An acoustic blanking zone about 500 m wide is observed on the corresponding sub-bottom profile (Fig. 6b). Two zones of enhanced amplitude occur within this acoustic blanking zone. On the top of the acoustic blanking zone, many diffraction events originate from seafloor domes. At the SE side, there is a zone where the seafloor reflection amplitude becomes very weak. This phenomenon is also observed on the multichannel seismic data (Fig. 6c). The multichannel seismic profile that passes through the drill site shows an anomalously strong amplitude at about 1 200 ms, which has been interpreted as the top of a buried relict venting system, and was confirmed to correspond to the occurrence of MDAC (Sha et al., 2015). The observed BSR is strong and discontinuous at this site. Below the BSR, chaotic reflections are abundant, manifesting the accumulation of free gas.

Site 09 was drilled near a small mound at a water depth of about 727 m (Fig. 7a). This mound is about 300 m in diameter and about 50 m high. Liu (2017) has proposed that this mound may have formed due to sediment expansion accompanying the formation of SGH, with a gas chimney acting as the gas migration pathway. The SBP (Fig. 7b) shows a about 150 m wide vertical zone of reduced amplitude, beneath the mound. Velocity pull-downs are observed at both sides of the vertical zone (Fig. 7b). Both the SBP and MCS data (Fig. 7c) show a weak seafloor reflection on the southeast side of the mound, similar to what was observed at site 08, associated with fluid venting at the seafloor.

Site16 was drilled on a topographic high at a water depth of about 871 m (Fig. 8a). The corresponding seismic profile shows a distinct continuous BSR near site 16 (Fig. 8c). The chaotic reflections below the BSR and seismic pull-downs are reliable indicators of free gas below the BSR. A reduced amplitude zone at the seafloor was observed on the SBP and MCS profiles, similar to sites 08 and 09 (Figs 8b and c).

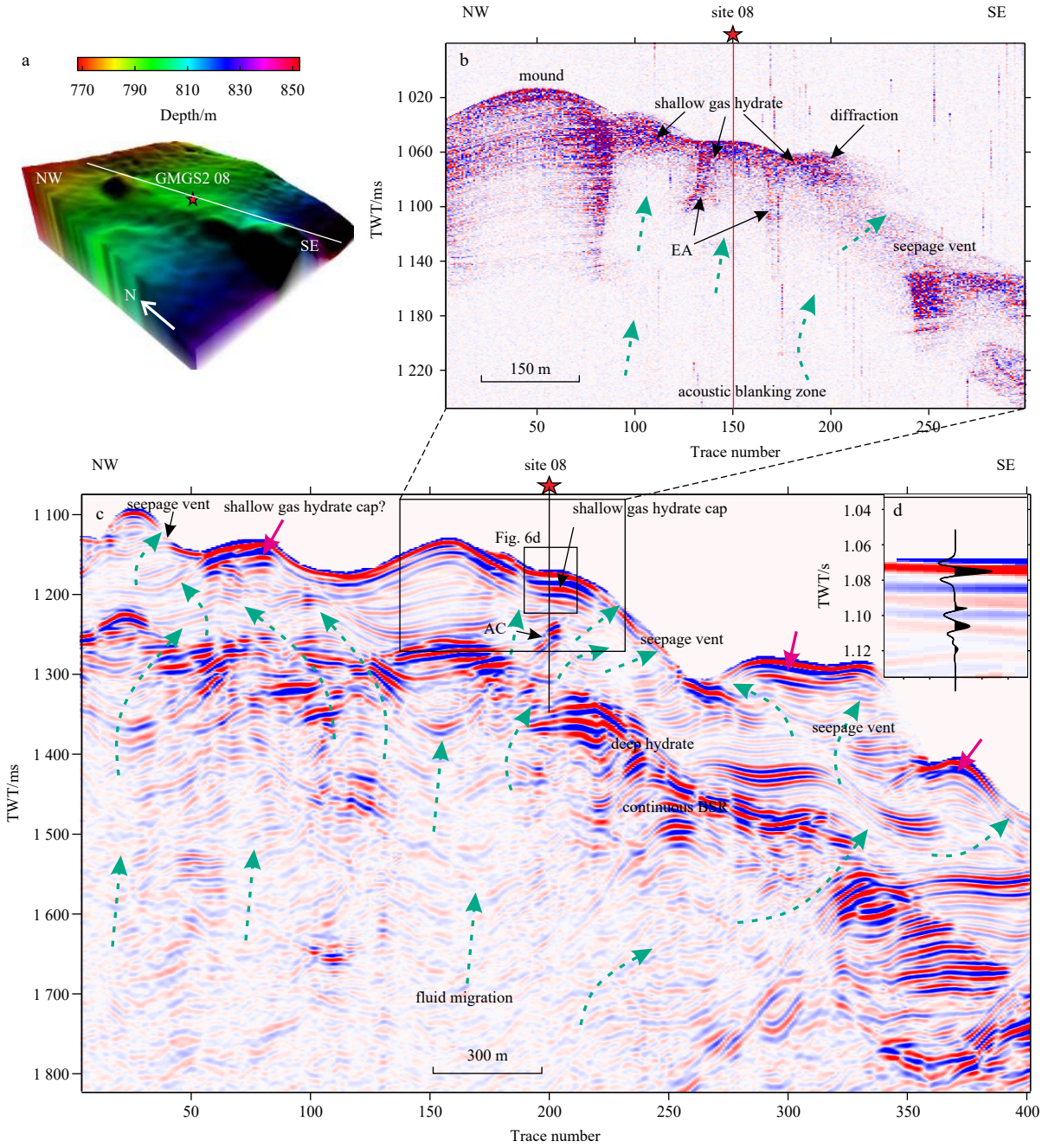


**Fig. 6.** Multibeam bathymetry (MB) (a), sub-bottom profiler (b) and multi-channel seismics (c) profiles crossing the site 08; synthetic seismogram (d) at the drill location of c. TWT: two-way-travel time, EA: enhanced amplitude, AC: authigenic carbonate, BSR: bottom simulating reflector. Green arrows indicate the inferred fluid flow pathways, and the red arrows may indicate the shallow gas hydrate caps. The grid interval of multi-beam bathymetric data is 50 m.

## 5 Discussion

The Chinese GMGS2 gas hydrate drilling program confirmed the occurrence of SGH in the Dongsha area. The drill cores and the geophysical logs together with the seismic sections provide an excellent opportunity to understand the characteristics and distribution of SGH and fluid migration pathways in this area. As listed in the Table 1, the shallow gas hydrate occurs at 8–30 m below the seafloor. Gas hydrates directly recovered from the seafloor have been reported at many drill sites in oceans around the world, but no such type of gas hydrate samples was observed in this area during this drilling program, nor during the previous R/V *SONNE 177* Cruise. Unlike the deep-seated gas hydrates which are disseminated in the fine to coarse-grained sediments with a concentration between 20% and 50% (Sha et al., 2015), the shallow gas hydrates are deposited in the silty clay (Zhang et al., 2014) with a higher concentration. The concentration of shallow gas hydrate can be up to 100% and are considered as pure gas hydrate (Sha et al., 2015). The differences in concentration are due to the different formation mechanisms. Shallow gas hydrates are associated with focused fluid flow while the deep-seated gas hydrates are associated with pervasive diffused fluid flow. The analysis of head-space gas and the gas from gas hydrate dissociation indicates a microbial source, though the contribution of a thermogenic source is also possible (Zhang et al., 2014).

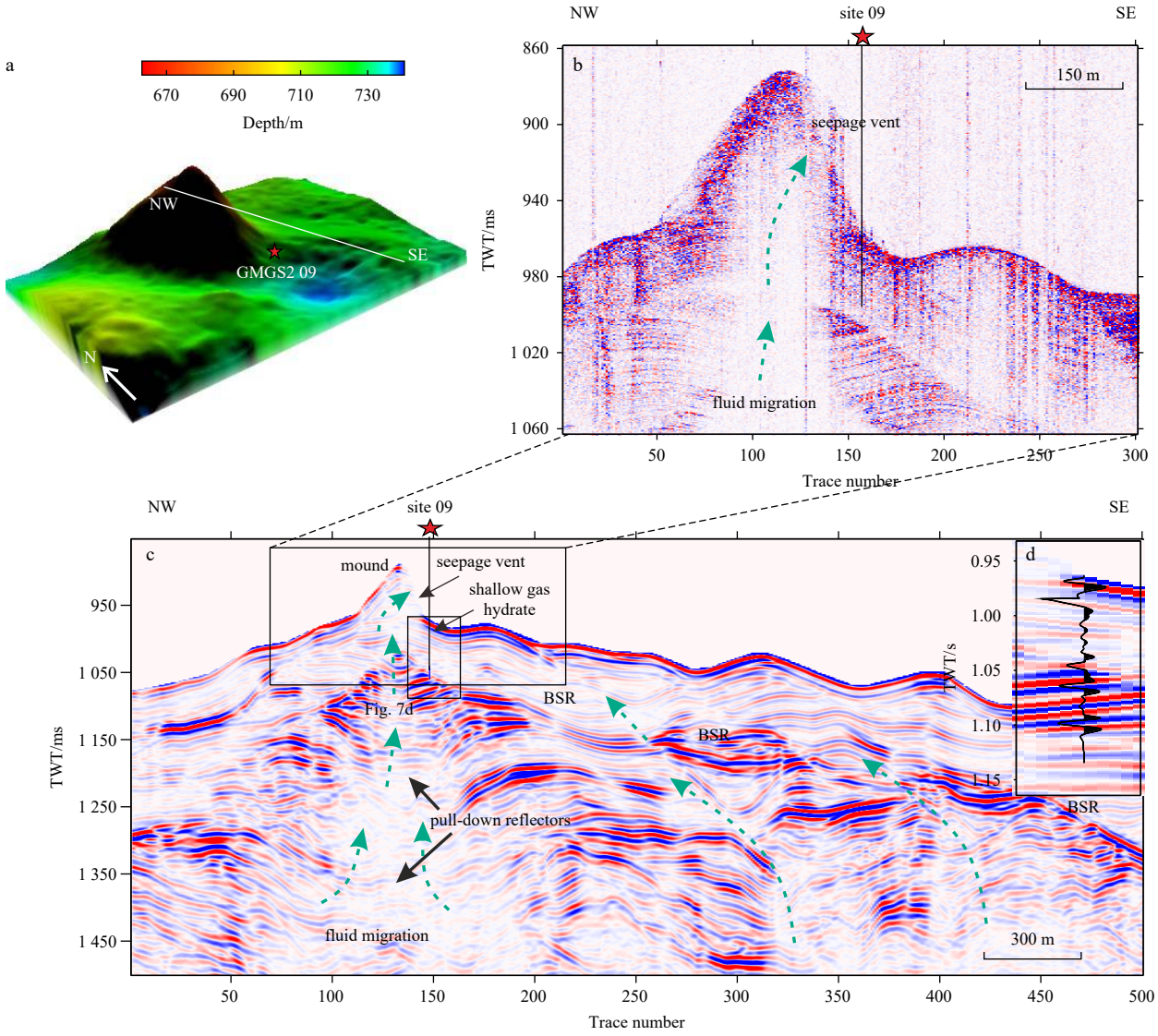


**Fig. 7.** Multibeam bathymetry (a), sub-bottom profiler (b) and multi-channel seismics (c) profiles crossing the site 09; synthetic trace (d) at the drill location of c. Green arrows indicate the inferred fluid flow pathways. TWT: two-way-travel time, BSR: bottom simulating reflector. The grid interval of multi-beam bathymetric data is 50 m.

### 5.1 *Characteristics of fluid migration pathways*

This study has recognized two main fluid migration pathways in the Dongsha area: gas chimneys and faults. Gas chimneys show different characteristics in SBP and MCS profiles. In the MCS profiles, they are usually interpreted according to vertical zones of reduced amplitudes (Figs 6c, 7c and 8c), representing major pathways for upward methane migration in the shallow sediments. Gas in gas chimneys usually induces seismic velocity pull downs or chaotic reflections, and make reflections weak or blank due to various contents. However, in SBP, gas chimneys are usually recognized as acoustic blanking zones, making layers discontinuous (Figs 6b, 7b and 8b). The gas chimneys characterized by acoustic blanking zones are abundant in the study area (Liu et al., 2015b). These patterns are coherent at each site (Figs 6b, 7b and 8b), indicating gas migration pathways and fluid escaping processes.

Gas chimneys were observed both below and above continuous and discontinuous BSRs. Continuous BSRs could serve as seal, altering the fluid migration pathways, since relative strong reflections occur in the GHSZ and weak or blank zones just below the BSRs (Figs 6c and 7c). Discontinuous BSRs are usually related to faults and fractures (Wang et al., 2014a). Therefore, in addition to gas chimneys, faults also act as the other pathways for upward migrating fluids. Submarine slides and mud volcanism activities cause abundant shallow faults and affect the seafloor morphology in the study area (Liu et al., 2015a). Unlike gas chimneys, faults act as favorable narrow gas pathways, with weak or blank reflections, linking gas pockets above and below the BSRs (Figs 6c, 7c and 8c).

Gases are usually accumulated in an acoustic blank area beneath the seafloor, with weak reflection zones at the seafloor. Seismic seafloor weak reflection zones are often interpreted as vent structures and the “soft”, recently extruded sediments frequently contain gas in bubble-phase (Roberts et al., 2006), where fluids seep into the ocean as vents. Such seepage vents are interpreted to result from active gas seepage rather than from gas bursts/sudden expulsions in the past, which would have likely caused residual seafloor pockmarks on the seafloor (Chen et al., 2015a, 2015b, 2018). The seepage vents observed at all three sites,

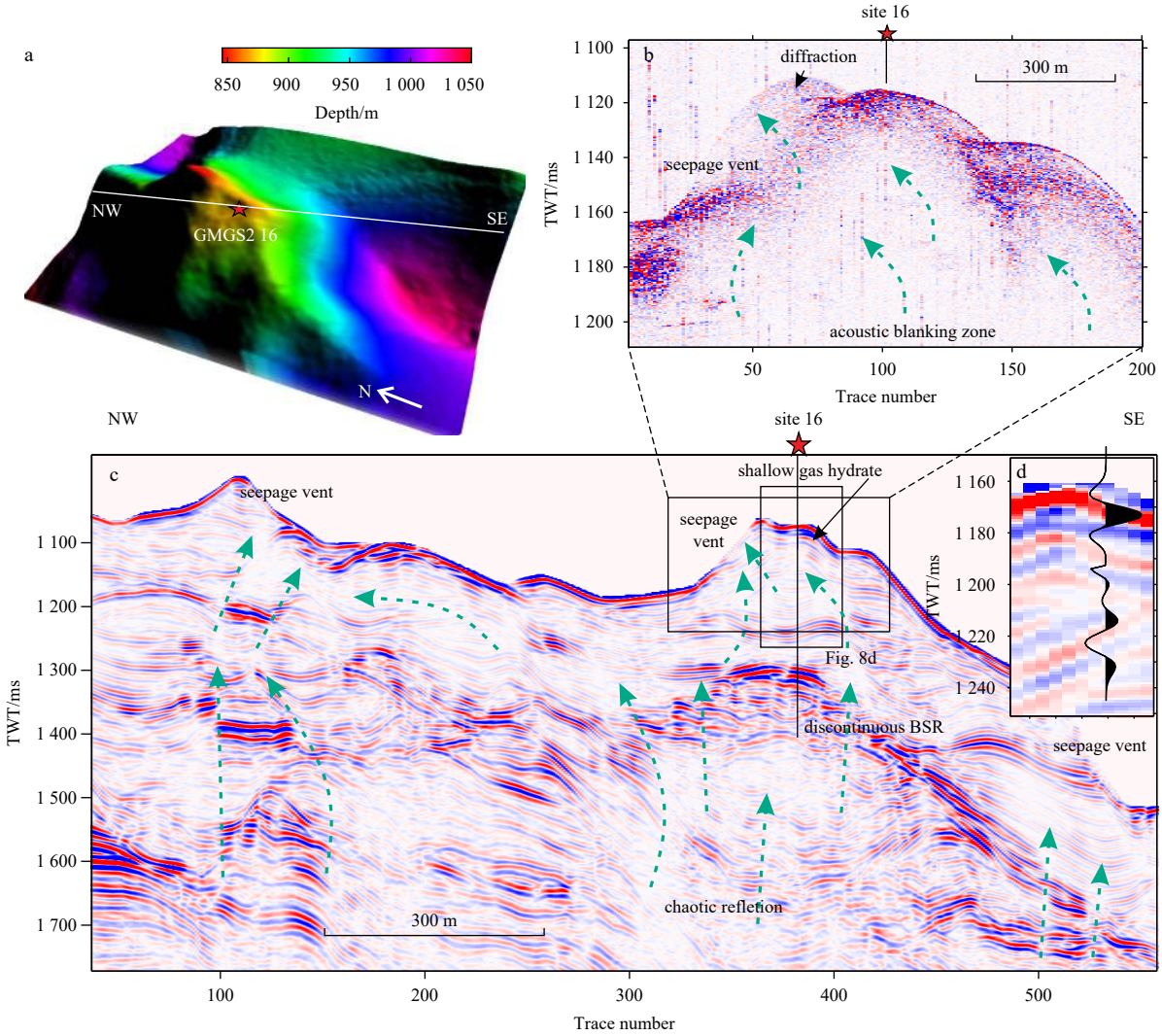


**Fig. 8.** Multibeam bathymetry (a), sub-bottom profiler (b) and multi-channel seismics (c) sections crossing the site 16; synthetic trace (d) at the drill location of c. Green arrows indicate the inferred fluid flow pathways. TWT: two-way-travel time, BSR: bottom simulating reflector. The grid interval of multi-beam bathymetric data is 50 m.

indicate the presence of fluid seepage. Since no gas bubble plumes (Liu et al., 2015b) have been captured on the SBP data, the seepage process could be weak and not easily detected in these sites. However, to form and maintain SGH, a high-flux of methane is needed (Foucher et al., 2009). The SMIs at sites 08 and 16 are much shallower than in the adjacent area (Wu et al., 2013), indicating these two sites are in higher-flux environment.

### 5.2 *Geophysical recognition of shallow gas hydrates*

The seismic velocity structure is one of the most used indicators in the exploration for deep gas hydrates and there are many successful examples (Boswell et al., 2016; Wang et al., 2018a). In the study area, seismic velocity anomalies were observed in the well logs at sites 08 and 16. At site 08, the seismic velocity of the hydrate-bearing sediment is as high as up to 2 600 m/s, therefore much higher than that for the background sediments at that depth. As such, velocity anomalies are the most reliable indicators also for SGH. However, it is very difficult to extract velocity information for small-scale bodies/occurrences. Another useful tool is resistivity. An anomalous zone, with a thickness of about 15 m, was observed at both sites 08 and 16. Resistivity logging, derived from CSEM (Controlled Source Electromagnetic) surveys has indeed been widely used to study cold seep systems and is a proven tool for the detection of SGH (Attias et al., 2016).

However, exploring for SGH without drilling and coring, is highly challenging, due to their small scale. No efficient method has yet been fully developed. Possible anomalies that could be used as indicators of SGH include: (1) seafloor reflection amplitude, (2) acoustic blanking zone supporting SGH; and (3) anomalies in seismic velocity and resistivity.

The presence of SGH may induce amplitude anomalies near the seafloor, since acoustic impedance will increase when sediments contains gas hydrates. Such amplitude anomalies have indeed been interpreted as gas hydrate accumulations elsewhere, such as in the Gulf of Mexico (Roberts et al., 2006). At sites 08 and 16, it could be found that the seafloor reflection is not a normal single event, but two or more in the MCS profiles (Figs 6c, 6d, 7c, 7d, 8c and 8d), and in the SBP, layers with SGH are dim or chaotic (Figs 6b, 7b and 8b). The presence of MDAC can also produce such amplitude anomalies. However, at site 16, dim layers also exist without MDAC at the seafloor, which means the reflections and the dim layers are most probably caused by the SGH close to

the seafloor.

SGH occur at the top of or around gas chimneys which are characterized by an acoustic blanking zone in the SBP. SGHs within gas chimneys have been inferred and/or recovered from many other places, such as the Nyegga pockmarks (Plaza-Faverola et al., 2010) and in the East Sea of Korea (Ryu et al., 2013). In the study sites, SGH are usually accompanied by fluid migration pathways and seepage venting at the seafloor. On one hand, this suggests SGH here are more likely to act as seals, altering the fluid migration pathways. On the other hand, it indicates that gas supply is high enough to support the SGH formation and sustainability. This confirms the study sites are in relatively high-flux environment.

### 5.3 *Relationship between shallow gas hydrates and cold seeps*

It is well recognized that the presence of gas hydrate is often associated with cold seep systems (Suess, 2014; Feng et al., 2018). This may also be a practical approach to infer the presence of SGH through the exploration of cold seep areas. Previous studies showed that cold seeps and gas chimneys manifested by acoustic blanking zones are abundant in this area (Liu et al., 2015b; Wang et al., 2018b), suggesting that SGH may be distributed widely in the Dongsha area. The connections between the occurrences of SGH and cold seeps are evident from the observation of reduced amplitudes vertical zones (gas chimneys and faults), seafloor weak reflection zones (seepage vent) and the presence of MDAC and SGH.

Based on the criteria discussed above, the migration pathways for gases in the study area are indicated in Figs 6b, 6c, 7b, 7c, 8b and 8c. Further, from the above analysis, it could be inferred that: (1) gases here usually migrate sinuously through gas chimneys and faults; (2) BSRs and the seafloor act as the two main seals for the migrating gas; (3) the majority of gases are trapped under the BSRs and a small amount of gases migrate into the GHSZ; and (4) gases gather in specific areas and seep through venting at the seafloor. SGH are controlled by the fluid migration pathways, which are greatly controlled by faults and deep-seated gas hydrates near the lower boundary of GHSZ. Gases seeping through active vents supply enough gas to sustain the SGH nearby, and therefore active cold seeps, either indicated by gas plumes or seepage vents, can also be used as indicators for neighboring SGH in the study area. From this aspect, SGH are important contributors to the venting gases (Chen et al., 2006) and may improve understanding of the thermodynamic disequilibrium system of hydrate, thereby deserving further investigation.

MDAC derived from the Anaerobic Oxidation of Methane process, are also indicators of past methane seepage (Magalhães et al., 2012). The formation of MDAC means that the cold seep is likely at the sealing stage (Hovland, 2002). As such, both SGH and MDAC can act as seals for free gas in the GHSZ. At site 09, the MDAC occur at the seafloor, suggesting they may have been recently formed. At site 08, however, the MDAC occur at about 9 m below the seafloor, below the SMI, suggesting they were most probably buried after formation. Multi-stage MDAC formation, confirmed by dating, indicates active and permanent migration of methane in this area. This is one of the critical conditions for gas hydrate formation and stabilization. However, MDAC formation at different depths in the sediments below seafloor, means that intensity of methane seepage was not constant throughout the geological periods. Although previous MDAC analyses in an adjacent area showed that most of the cold seeps were not recently active (at least since 11.5 ka before present) (Tong et al., 2013; Han et al., 2014), present fluid migration pathways and shallow gas formation indicate that active gas leakage is moving through seepage vents at a relatively high-flux state, but not resulting in gas plumes easily detected by acoustic exploration.

## 6 Conclusions

The presence of the SGH has been confirmed by drilling cores at three sites during the GMGS2 Cruise, in the scope of China's second gas hydrate drilling program. The recovered SGH occur as veins, blocky nodules or massive layers at 8–30 m below the seafloor in the study sites, in the northern South China Sea.

The seismic velocities and resistivities of the shallow hydrate-bearing sediments are high, although much lower than those associated with the deep-seated gas hydrates, thereby proving useful tools for their detection. In addition, at the seafloor, two or more reflections in the high-resolution seismic profiles and dim or chaotic layers in the sub-bottom profiles are also most likely indicators of SGH.

The occurrence of SGH is spatially associated with the presence of cold seep areas and associated ecosystems. Gas chimneys and faults are two main observed fluid migration pathways for cold seeps in the Dongsha area. The coherent patterns of gas chimneys at the three sites investigated, indicate they acted as major gas migration pathways. BSRs and the shallow hydrate-bearing sediments act as the two main seals for the migrating gas, and the SGH are controlled by the fluid migration pathways, which are controlled in turn by faults and occurrences of deep-seated gas hydrates at the base of GHSZ. Present fluid migration pathways and shallow gas formation indicate that active gas leakage is seeping through vents in a relatively high-flux state, but not resulting in gas plumes easily detectable by acoustic exploration. As such, active cold seeps, either indicated by gas plumes or seepage vents, can be used as indicators for neighboring SGH in the study area. Finally, multi-stage formation of MDAC in the study area indicates active and permanent migration of methane, but the intensity of methane seepage was not constant in individual geological periods.

As a final conclusion, the widely distributed gas chimneys and seepage vents in the Dongsha area, identified with geophysical methods, indicate the widespread occurrence of SGH close to the seafloor, confirmed by drilling and logging results. Further work needs to be done to confirm more SGH occurrences detected using the criteria defined here, and also to better understand the complex fluid escape and gas hydrate formation/accumulation processes, essential to fully evaluate the potential for gas hydrate exploration and exploitation in the Dongsha area.

### *Acknowledgements*

We thank Guangzhou Marine Geological Survey for their permission to release the geophysical data. Luis M. Pinheiro thanks FCT/MCTES for the financial support to CESAM (UID/AMB/50 017 /2019), through national funds. Thanks to the two anonymous reviewers for their constructive comments.

## References

Attias E, Weitemeyer K, Minshull T A, et al. 2016. Controlled-source electromagnetic and seismic delineation of subseafloor fluid flow structures in a gas hydrate province, offshore Norway. Geophysical Journal International, 206(2): 1093–1110, doi: 10.1093/gji/ggw188

Bahk J J, Kim J H, Kong G S, et al. 2009. Occurrence of near-seafloor gas hydrates and associated cold vents in the Ulleung Basin, East Sea. Geosciences Journal, 13(4): 371–385, doi: 10.1007/s12303-009-0039-8

Bangs N L B, Sawyer D S, Golovchenko X. 1993. Free gas at the base of

the gas hydrate zone in the vicinity of the Chile triple junction. Geology, 21(10): 905–908, doi: 10.1130/0091-7613(1993)021<0905:FGATBO>2.3.CO;2

Berndt C, Bunz S, Clayton T, et al. 2004. Seismic character of bottom simulating reflectors: examples from the mid-Norwegian margin. Marine and Petroleum Geology, 21(6): 723–733, doi: 10.1016/j.marpetgeo.2004.02.003

Boswell R, Collett T S. 2011. Current perspectives on gas hydrate resources. Energy & Environmental Science, 4(4): 1206–1215

Boswell R, Shipp C, Reichel T, et al. 2016. Prospecting for marine gas hydrate resources. Interpretation, 4(1): SA13–SA24, doi: 10.1190/INT-2015-0036.1

Chen Duofu, Huang Yongyang, Yuan Xunlai, et al. 2005. Seep carbonates and preserved methane oxidizing archaea and sulfate reducing bacteria fossils suggest recent gas venting on the seafloor in the northeastern South China Sea. Marine and Petroleum Geology, 22(5): 613–621, doi: 10.1016/j.marpetgeo.2005.05.002

Chen Duofu, Su Zheng, Cathles L M. 2006. Types of gas hydrates in marine environments and their thermodynamic characteristics. Terrestrial, Atmospheric and Oceanic Sciences, 17(4): 723–737, doi: 10.3319/TAO.2006.17.4.723(GH)

Chen Fang, Hu Yu, Feng Dong, et al. 2016. Evidence of intense methane seepages from molybdenum enrichments in gas hydrate-bearing sediments of the northern South China Sea. Chemical Geology, 443: 173–181, doi: 10.1016/j.chemgeo.2016.09.029

Chen Jiangxin, Guan Yongxian, Song Haibin, et al. 2015a. Distribution characteristics and geological implications of pockmarks and mud volcanoes in the northern and western continental margins of the South China Sea. Chinese Journal of Geophysics (in Chinese), 58(3): 919–938

Chen Jiangxin, Song Haibin, Guan Yongxian, et al. 2015b. Morphologies, classification and genesis of pockmarks, mud volcanoes and associated fluid escape features in the northern Zhongjiannan Basin, South China Sea. Deep Sea Research Part Ⅱ: Topical Studies in Oceanography, 122: 106–117, doi: 10.1016/j.dsr2.2015.11.007

Chen Jiangxin, Song Haibin, Guan Yongxian, et al. 2018. Geological and oceanographic controls on seabed fluid escape structures in the northern Zhongjiannan Basin, South China Sea. Journal of Asian Earth Sciences, 168: 8–47

Etiope G, Milkov A V, Derbyshire E. 2008. Did geologic emissions of methane play any role in Quaternary climate change?. Global and Planetary Change, 61(1–2): 79–88, doi: 10.1016/j.gloplacha.2007.08.008

Feng Dong, Chen Duofu. 2015. Authigenic carbonates from an active cold seep of the northern South China Sea: New insights into fluid sources and past seepage activity. Deep Sea Research Part Ⅱ: Topical Studies in Oceanography, 122: 74–83, doi: 10.1016/j.dsr2.2015.02.003

Feng Dong, Qiu Jianwen, Hu Yu, et al. 2018. Cold seep systems in the South China Sea: An overview. Journal of Asian Earth Sciences, 168: 3–16, doi: 10.1016/j.jseaes.2018.09.021

Foucher J P, Westbrook G K, Boetius A, et al. 2009. Structure and drivers of cold seep ecosystems. Oceanography, 22(1): 92–109, doi: 10.5670/oceanog.2009.11

Gardner J M. 2001. Mud volcanoes revealed and sampled on the western moroccan continental margin. Geophysical Research Letters, 28(2): 339–342, doi: 10.1029/2000GL012141

Han Xiqiu, Suess E, Huang Yongyang, et al. 2008. Jiulong methane reef: Microbial mediation of seep carbonates in the South China Sea. Marine Geology, 249(3–4): 243–256, doi: 10.1016/j.margeo.2007.11.012

Han Xiqiu, Suess E, Liebetrau V, et al. 2014. Past methane release events and environmental conditions at the upper continental slope of the South China Sea: constraints by seep carbonates. International Journal of Earth Science, 103(7): 1873–1887, doi: 10.1007/s00531-014-1018-5

Hovland M. 2002. On the self-sealing nature of marine seeps. Continental Shelf Research, 22(16): 2387–2394, doi: 10.1016/S0278-4343(02)00063-8

Huang Chiyue, Chien C W, Zhao Meixun, et al. 2006. Geological study of active cold seeps in the syn-collision accretionary prism Kaoping slope off SW Taiwan. Terrestrial, Atmospheric and Oceanic Sciences, 17(4): 679–702, doi: 10.3319/TAO.2006.17.4.679(GH)

Hyndman R D, Spence G D. 1992. A seismic study of methane hydrate marine bottom simulating reflectors. Journal of Geophysical Research: Solid Earth, 97(B5): 6683–6698, doi: 10.1029/92JB00234

Kvenvolden K A. 1993. Gas hydrates-geological perspective and global change. Reviews of Geophysics, 31(2): 173–187, doi: 10.1029/93RG00268

Li Jinfa, Ye Jianliang, Qin Xuwen, et al. 2018. The first offshore natural gas hydrate production test in South China Sea. China Geology, 1(1): 5–16, doi: 10.31035/cg2018003

Li Lun, Lei Xinhua, Zhang Xin, et al. 2013. Gas hydrate and associated free gas in the Dongsha Area of northern South China Sea. Marine and Petroleum Geology, 39(1): 92–101, doi: 10.1016/j.marpetgeo.2012.09.007

Li Niu, Feng Dong, Chen Linying, et al. 2016. Using sediment geochemistry to infer temporal variation of methane flux at a cold seep in the South China Sea. Marine and Petroleum Geology, 77: 835–845, doi: 10.1016/j.marpetgeo.2016.07.026

Liu Bin. 2017. Gas and gas hydrate distribution around seafloor mound in the Dongsha area, north slope of the South China Sea. Haiyang Xuebao (in Chinese), 39(3): 68–75

Liu Boran, Song Haibin, Guan Yongxian, et al. 2015a. Submarine slide and mud volcanism activities in gas hydrate bearing area on the northeastern slope, South China Sea. Haiyang Xuebao (in Chinese), 37(9): 59–70

Liu Boran, Song Haibin, Guan Yongxian, et al. 2015b. Characteristics and formation mechanism of cold seep system in the northeastern continental slope of South China Sea from sub-bottom profiler data. Chinese Journal of Geophysics (in Chinese), 58(1): 247–256

Lu Hongfeng, Liu Jian, Chen Fang, et al. 2005. Mineralogy and stable isotopic composition of authigenic carbonates in bottom sediments in the offshore area of southwest Taiwan, South China Sea: Evidence for gas hydrates occurrence. Earth Science Frontiers (in Chinese), 12(3): 268–276

MacDonald I R, Bender L C, Vardaro M, et al. 2005. Thermal and visual time-series at a seafloor gas hydrate deposit on the Gulf of Mexico slope. Earth and Planetary Science Letters, 233(1–2): 45–59, doi: 10.1016/j.epsl.2005.02.002

MacDonald I R, Guinasso N L Jr, Sassen R, et al. 1994. Gas hydrate that breaches the sea floor on the continental slope of the Gulf of Mexico. Geology, 22(8): 699–702, doi: 10.1130/0091-7613(1994)022<0699:GHTBTS>2.3.CO;2

MacKay M E, Jarrard R D, Westbrook G K, et al. 1994. Origin of bottom-simulating reflectors: Geophysical evidence from the Cascadia accretionary prism. Geology, 22(5): 459–462, doi: 10.1130/0091-7613(1994)022<0459:OOBSRG>2.3.CO;2

Magalhães V H, Pinheiro L M, Ivanov M K, et al. 2012. Formation processes of methane-derived authigenic carbonates from the gulf of Cadiz. Sedimentary Geology, 243–244: 155–168, doi: 10.1016/j.sedgeo.2011.10.013

Mazurenko L L, Soloviev V A, Belenkaya I, et al. 2002. Mud volcano gas hydrates in the gulf of Cadiz. Terra Nova, 14(5): 321–329, doi: 10.1046/j.1365-3121.2002.00428.x

McDonnell S L, Max M D, Cherkis N Z, et al. 2000. Tectono-sedimentary controls on the likelihood of gas hydrate occurrence near Taiwan. Marine and Petroleum Geology, 17(8): 929–936, doi: 10.1016/S0264-8172(00)00023-4

Petersen C J, Papenberg C, Klaeschen D. 2007. Local seismic quantification of gas hydrates and BSR characterization from multi-frequency OBS data at northern Hydrate Ridge. Earth and Planetary Science Letters, 255(3–4): 414–431, doi: 10.1016/j.epsl.2007.01.002

Pinheiro L M, Ivanov M K, Sautkin A, et al. 2003. Mud volcanism in the Gulf of Cadiz: results from the TTR-10 cruise. Marine Geology, 195(1–4): 131–151, doi: 10.1016/S0025-3227(02)00685-0

Plaza-Faverola A, Westbrook G K, Ker S, et al. 2010. Evidence from three-dimensional seismic tomography for a substantial accumulation of gas hydrate in a fluid-escape chimney in the Nyegga pockmark field, offshore Norway. Journal of Geophysical Research: Solid Earth, 115(B8): B08104

Reagan M T, Moridis G J. 2007. Oceanic gas hydrate instability and dissociation under climate change scenarios. Geophysical Research Letters, 34(22): L22709, doi: 10.1029/2007GL031671

Riedel M. 2007. 4D seismic time-lapse monitoring of an active cold vent, northern Cascadia margin. Marine Geophysical Researches, 28(4): 355–371, doi: 10.1007/s11001-007-9037-2

Riedel M, Novosel I, Spence G D, et al. 2006. Geophysical and geochemical signatures associated with gas hydrate-related venting in the northern Cascadia margin. GSA Bulletin, 118(1–2): 23–38, doi: 10.1130/B25720.1

Roberts H H, Hardage B A, Shedd W W, et al. 2006. Seafloor reflectivity—an important seismic property for interpreting fluid/gas expulsion geology and the presence of gas hydrate. The Leading Edge, 25(5): 620–628, doi: 10.1190/1.2202667

Ruppel C D, Kessler J D. 2017. The interaction of climate change and methane hydrates. Reviews of Geophysics, 55(1): 126–168, doi: 10.1002/2016RG000534

Ryu B J, Collett T S, Riedel M, et al. 2013. Scientific results of the Second Gas Hydrate Drilling Expedition in the Ulleung Basin (UBGH2). Marine and Petroleum Geology, 47: 1–20, doi: 10.1016/j.marpetgeo.2013.07.007

Sha Zhibin, Liang Jinqiang, Zhang Guangxue, et al. 2015. A seepage gas hydrate system in northern South China Sea: Seismic and well log interpretations. Marine Geology, 366: 69–78, doi: 10.1016/j.margeo.2015.04.006

Shedd W, Boswell R, Frye M. 2012. Occurrence and nature of "bottom simulating reflectors" in the northern Gulf of Mexico. Marine and Petroleum Geology, 34(1): 31–40, doi: 10.1016/j.marpetgeo.2011.08.005

Shipley T, Houston M H, Buffler R T, et al. 1979. Seismic evidence for widespread possible gas hydrate horizons on continental slopes and rises. AAPG Bulletin, 63(12): 2204–2213

Shyu C T, Hsu S K, Liu C S. 1998. Heat flows off southwest Taiwan: Measurements over mud diapirs and estimated from bottom simulating reflectors. Terrestrial, Atmospheric and Oceanic Sciences, 9(4): 795–812, doi: 10.3319/TAO.1998.9.4.795(TAICRUST)

Suess E. 2014. Marine cold seeps and their manifestations: geological control, biogeochemical criteria and environmental conditions. International Journal of Earth Sciences, 103(7): 1889–1916, doi: 10.1007/s00531-014-1010-0

Suess E, Torres M E, Bohrmann G, et al. 2001. Sea floor methane hydrates at Hydrate Ridge, Cascadia. In: Paull C K, Dillon W P, eds. Natural Gas Hydrates: Occurrence, Distribution, and Detection. American: AGU, 87–98

Tong Hongpeng, Feng Dong, Cheng Hai, et al. 2013. Authigenic carbonates from seeps on the northern continental slope of the South China Sea: New insights into fluid sources and geochronology. Marine and Petroleum Geology, 43: 260–271, doi: 10.1016/j.marpetgeo.2013.01.011

Vanneste M, Sultan N, Garziglia S, et al. 2014. Seafloor instabilities and sediment deformation processes: The need for integrated, multi-disciplinary investigations. Marine Geology, 352: 183–214, doi: 10.1016/j.margeo.2014.01.005

Wang Jiliang, Jaiswal P, Haines S S, et al. 2018a. Gas hydrate quantification using full-waveform inversion of sparse ocean-bottom seismic data: A case study from Green Canyon Block 955, Gulf of Mexico. Geophysics, 83(4): B167–B181, doi: 10.1190/geo2017-0414.1

Wang Jiliang, Sain K, Wang Xiujuan, et al. 2014a. Characteristics of bottom-simulating reflectors for Hydrate-filled fractured sediments in Krishna-Godavari Basin, eastern Indian margin. Journal of Petroleum Science and Engineering, 122: 515–523, doi: 10.1016/j.petrol.2014.08.014

Wang Jiliang, Wu Shiguo, Kong Xiu, et al. 2018b. Subsurface fluid flow at an active cold seep area in the Qiongdongnan Basin, northern South China Sea. Journal of Asian Earth Sciences, 168: 17–26, doi: 10.1016/j.jseaes.2018.06.001

Wang Jiliang, Wu Shiguo, Yao Yongjian. 2018c. Quantifying gas hydrate from microbial methane in the South China Sea. Journal of Asian Earth Sciences, 168: 48–56, doi: 10.1016/j.jseaes.2018.01.020

Wang Shuhong, Yan Wen, Magalhães V H, et al. 2012. Calcium isotope fractionation and its controlling factors over authigenic carbonates in the cold seeps of the northern South China Sea. Chinese Science Bulletin, 57(11): 1325–1332, doi: 10.1007/s11434-012-4990-9

Wang Shuhong, Yan Wen, Magalhães V H, et al. 2014b. Factors influencing methane-derived authigenic carbonate formation at cold seep from southwestern Dongsha area in the northern South China Sea. Environmental Earth Sciences, 71(5): 2087–2094, doi: 10.1007/s12665-013-2611-9

Wang Xiujuan, Liu Bo, Qian Jin, et al. 2018d. Geophysical evidence for gas hydrate accumulation related to methane seepage in the Taixinan Basin, South China Sea. Journal of Asian Earth Sciences, 168: 27–37, doi: 10.1016/j.jseaes.2017.11.011

Wenau S, Spiess V, Pape T, et al. 2015. Cold seeps at the salt front in the lower Congo Basin I: Current methane accumulation and active seepage. Marine and Petroleum Geology, 67: 894–908, doi: 10.1016/j.marpetgeo.2014.07.032

Wu Lushan, Yang Shengxiong, Liang Jinqiang, et al. 2013. Variations of pore water sulfate gradients in sediments as indicator for underlying gas hydrate in Shenhu Area, the South China Sea. Science China Earth Sciences, 56(4): 530–540, doi: 10.1007/s11430-012-4545-6

Yan Pin, Deng Hui, Liu Hailing. 2006. The geological structure and prospect of gas hydrate over the Dongsha Slope, South China Sea. Terrestrial, Atmospheric and Oceanic Sciences, 17(4): 645–658, doi: 10.3319/TAO.2006.17.4.645(GH)

Yang Shengxiong, Zhang Ming, Liang Jinqiang, et al. 2015. Preliminary results of China's third gas hydrate drilling expedition: A critical step from discovery to development in the South China Sea. Fire in the Ice: Methane Hydrate Newsletter, 15(2): 1–5

Zhang Guangxue, Yang Shengxiong, Zhang Ming, et al. 2014. GMGS2 expedition investigates rich and complex gas hydrate environment in the South China Sea. Fire in the Ice: Methane Hydrate Newsletter, 14(1): 1–5

Zhang Haiqi, Yang Shengxiong, Wu Nengyou, et al. 2007. China's first gas hydrate expedition successful. Fire in the Ice: Methane Hydrate Newsletter, 7(2): 1

Zhuang Chang, Chen Fang, Cheng Sihai, et al. 2016. Light carbon isotope events of foraminifera attributed to methane release from gas hydrates on the continental slope, northeastern South China Sea. Science China Earth Sciences, 59(10): 1981–1995, doi: 10.1007/s11430-016-5323-7